A curved shell finite element for the geometrically non-linear analysis of box-girder beams curved in plan

Ülkü H. Çalık-Karaköse[*1], Engin Orakdöğen[1], Ahmet I. Saygun[1] and Harm Askes[2]

[1]*Department of Civil Engineering, Faculty of Civil Engineering, Istanbul Technical University,
34469 Maslak, İstanbul, Turkey*
[2]*Department of Civil and Structural Engineering, University of Sheffield,
Sir Frederick Mappin Building Mappin Street, Sheffield, S1 3JD, U.K.*

Abstract.   A four-noded curved shell finite element for the geometrically non-linear analysis of beams curved in plan is introduced. The structure is conceived as a sequence of macro-elements (ME) having the form of transversal segments of identical topology where each slice is formed using a number of the curved shell elements which have 7 degrees of freedom (DOF) per node. A curved box-girder beam example is modelled using various meshes and linear analysis results are compared to the solutions of a well-known computer program SAP2000. Linear and non-linear analyses of the beam under increasing uniformly distributed loads are also carried out. In addition to box-girder beams, the proposed element can also be used in modelling open-section beams with curved or straight axes and circular plates under radial compression. Buckling loads of a circular plate example are obtained for coarse and successively refined meshes and results are compared with each other. The advantage of this element is that curved systems can be realistically modelled and satisfactory results can be obtained even by using coarse meshes.

Keywords: curved shell finite element; second-order effect; buckling

1. Introduction

Bridges with box-girder sections have been widely preferred especially due to their relatively high torsional stiffness. Torsional stiffness is important for straight bridges in distribution of eccentric loads more effectively in cross-sectional direction and also for curved bridges which can be subjected to significant torsional effects.

Cross-section types for box-girder bridges constructed to date are single-cell, multicell, and multispine box sections with rectangular or trapezoidal shapes. Analyses of single-cell and multi-cell box girders have been made using folded plate or shell elements (Meyer and Scordelis 1971, Fam and Turkstra 1975, Moffat and Lim 1977) and using box beam elements considering flexural, torsional and distortional behaviours of box girders as given in Razaqpur and Li (1991). In Park *et al*. (2005), a thin-walled box beam element for straight box girder bridges has been developed and an eccentric loading was decomposed into flexural, torsional and distortional forces by using the

---

*Corresponding author, Ph.D., E-mail: calikkarakose@itu.edu.tr

force equilibrium in order to consider the distortional behaviour of the multicell box girders independently. In Zhang and Lyons (1984), the thin-walled beam theory has been directly combined with the finite element technique to provide a new thin-walled box beam element which includes three extra degrees-of-freedom over the normal six degrees-of-freedom beam formulation, to take into account the warping and distortional effects.

It is normally impossible to construct bridges entirely with straight axes. Therefore, designing some parts or all of the system with a curved axis becomes inevitable (Zhang and Lyons 1984, Hiroshi and Chai 1988, Hall 1996, Zureick *et al*. 2000, Razaqpur and Li 1994, 1997). An efficient finite segment method for the analysis of curved box girders with corner stiffeners was presented in Wang *et al*. (2005). A more exact horizontally curved beam finite element in which the true warping degree of freedom conforms to the bimoment was developed in Hsu *et al*. (1990) where the beam element can be used for both open and closed sections. Experimental studies of curved beams were also carried out by some researchers as in Zureick *et al*. (2000), Shanmugam *et al*. (1995).

Second order effects gain importance for systems with thin walls like steel bridges and they need to be taken into consideration in order to make more realistic analysis. These effects are taken into account in Erkmen and Bradford (2009) where a total Lagrangian finite element formulation for the elastic analysis of steel-concrete composite beams that are curved in plan is developed. A displacement-based one-dimensional finite element model with geometric nonlinearity is introduced for thin-walled composite box beams and also for general thin-walled open-section composite beams in (Vo and Lee 2009, 2010) and a finite element model of spatial thin-walled beams with general open cross section is presented in Wang and Yang (2009).

Triangular or quadrilateral finite elements are generally used in the modelling of curved bridges in the literature, see for instance Moffat and Lim (1977). However, significant errors may occur from the usage of coarse meshes due to the straight edges of the elements. Thus, very fine meshes need to be used to be able to model the curved parts of the system realistically which increase the computational cost. Using a curved element instead, enables the usage of coarse meshes in design which is more convenient.

Developing such a curved finite element is the objective of the present paper. The proposed curved shell finite element has 7 degrees of freedom at each node and the shape functions and their derivatives are of a high polynomial degree. Thus, the element meets the expectations as satisfactory results can be obtained by using coarse meshes and geometrically non-linear analyses of thin walled open and closed section systems can be carried out by the inclusion of the second order effects, as will be illustrated with numerical examples.

2. Curved shell finite element

A segment of a curved box girder bridge modelled with a typical curved shell finite element discretization is shown in Fig. 1.

Geometrical properties of the curved shell finite element with circular cross-section and the directions of the displacement parameters *u, v* and *w* are shown in Fig. 2. *u* and *v* indicate the displacements in *s* and θ directions and *w* shows the displacement perpendicular to the element

The elevation coordinate *r* is related to the coordinate *s*, the elevation coordinate R_o of the origin and the slope angle ϕ by which the elevation coordinates R_1 and R_2 of the element edges can also be determined, that is
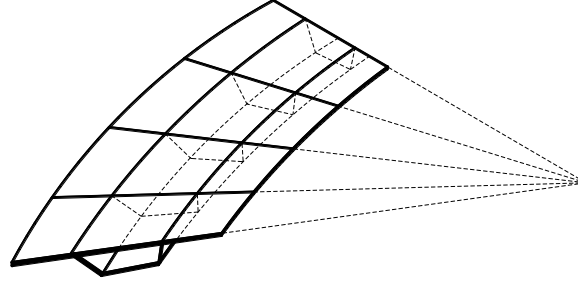
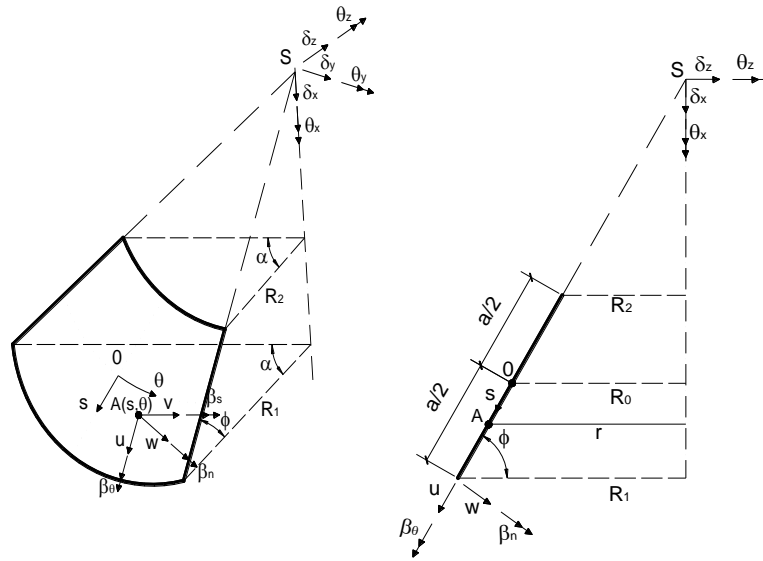Fig. 1 Box girder bridge segment with curved axis and its finite element mesh

Fig. 2 3D(left) view and vertical section (right) of the curved shell finite element

$$r = R_o + s\cos\phi$$

$$R_1 = R_o + \frac{a}{2}\cos\phi$$

$$R_2 = R_o - \frac{a}{2}\cos\phi \tag{1}$$

The curved shell element can also be transformed into a ring sector element and a cylindrical element by setting the slope angle ϕ to 0° and 90°, respectively.

2.1 Displacement functions and deformation field

Defining any rigid displacement of the curved shell element in space depending on the translation and rotation components of point S, the displacements at any point can be expressed as

$$
\begin{bmatrix} u \\ v \\ w \end{bmatrix}_R = \begin{bmatrix} \sin\phi & \sin\theta\cos\phi & -\cos\theta\cos\phi & 0 & 0 & 0 \\ 0 & \cos\theta & \sin\theta & -r & r\sin\theta\tan\phi & -r\cos\theta\tan\phi \\ \cos\phi & -\sin\theta\sin\phi & \cos\theta\sin\phi & 0 & r\cos\theta/\cos\phi & r\sin\theta/\cos\phi \end{bmatrix} \begin{bmatrix} \delta_x \\ \delta_y \\ \delta_z \\ \theta_x \\ \theta_y \\ \theta_z \end{bmatrix} \quad (2)
$$

which have trigonometric functions in terms of the variable θ.

Membrane internal force variations in longitudinal direction gain importance in curved box girder beams. Thus, equivalent 3rd order auxiliary shape functions ($a_1+a_2+a_3\cos\theta+a_4\sin\theta$) are used as u and v displacement functions in θ direction to be able to represent the actual displacement and internal force distributions sufficiently. Although curvatures and bending moments are negligible in θ direction, equivalent 3rd order auxiliary shape functions are also used for w in order to provide the displacement continuity along the common edges of elements connected with different angles. Linear auxiliary shape functions are used in s direction for u and v while 3rd order functions are used for w since β_s is the derivative of w with respect to s. Equivalent linear auxiliary shape functions ($c_1\cos\theta+c_2\sin\theta$) are used in θ direction for the freedom β_s.

Auxiliary shape functions and corresponding boundary conditions of the curved shell finite element are given in Table 1 where $l_i(s)$ and $\lambda_i(\theta)$ indicate linear and $f_i(s)$, $g_i(s)$, $\varphi_i(\theta)$ and $\psi_i(\theta)$ indicate 3rd order variations.

The element nodes and their freedoms are given in Fig. 3. The directions of the degrees of freedom are different from the local element axes and they only coincide for the special condition $\phi=0°$.

The defined axis system is common for all elements connected with different slope angles. Thus, axis transformations will not be necessary in the assembly process of system stiffness matrices from element stiffness matrices.

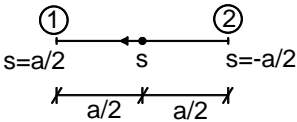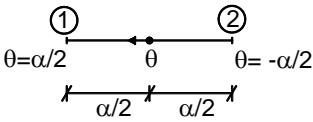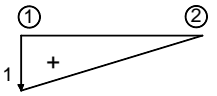Table 1 Auxiliary shape functions and boundary conditions of curved shell finite element
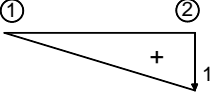
Function	Boundary condition	Shape
$l_1(s)=\dfrac{1}{2}+\dfrac{s}{a}$	$s=\dfrac{a}{2}\rightarrow l_1=1$ $s=-\dfrac{a}{2}\rightarrow l_1=0$	
$l_2(s)=\dfrac{1}{2}-\dfrac{s}{a}$	$s=\dfrac{a}{2}\rightarrow l_2=0$ $s=-\dfrac{a}{2}\rightarrow l_2=1$	

Table 1 Continued
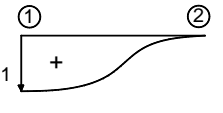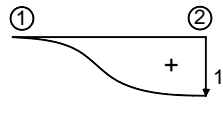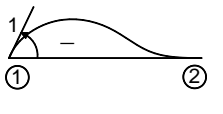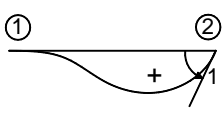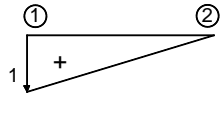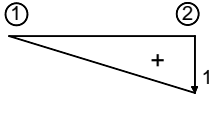
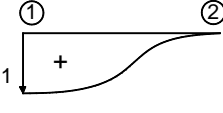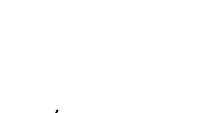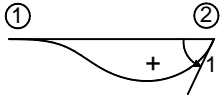|		
$f_1(s) = \dfrac{1}{2} + \dfrac{3s}{2a} - \dfrac{2s^3}{a^3}$	$s = \dfrac{a}{2} \rightarrow f_1 = 1; \dfrac{\partial f_1}{\partial s} = 0$ $s = -\dfrac{a}{2} \rightarrow f_1 = 0; \dfrac{\partial f_1}{\partial s} = 0$	
$f_2(s) = \dfrac{1}{2} - \dfrac{3s}{2a} + \dfrac{2s^3}{a^3}$	$s = \dfrac{a}{2} \rightarrow f_2 = 0; \dfrac{\partial f_2}{\partial s} = 0$ $s = -\dfrac{a}{2} \rightarrow f_2 = 1; \dfrac{\partial f_2}{\partial s} = 0$	
$g_1(s) = -\dfrac{a}{8} - \dfrac{s}{4} + \dfrac{s^2}{2a} + \dfrac{s^3}{a^2}$	$s = \dfrac{a}{2} \rightarrow g_1 = 0; \dfrac{\partial g_1}{\partial s} = 1$ $s = -\dfrac{a}{2} \rightarrow g_1 = 0; \dfrac{\partial g_1}{\partial s} = 0$	
$g_2(s) = \dfrac{a}{8} - \dfrac{s}{4} - \dfrac{s^2}{2a} + \dfrac{s^3}{a^2}$	$s = \dfrac{a}{2} \rightarrow g_2 = 0; \dfrac{\partial g_2}{\partial s} = 0$ $s = -\dfrac{a}{2} \rightarrow g_2 = 0; \dfrac{\partial g_2}{\partial s} = 1$	
$\lambda_1(\theta) = \dfrac{\cos\theta}{2\cos\dfrac{\alpha}{2}} + \dfrac{\sin\theta}{2\sin\dfrac{\alpha}{2}}$	$\theta = \dfrac{\alpha}{2} \rightarrow \lambda_1 = 1$ $\theta = -\dfrac{\alpha}{2} \rightarrow \lambda_1 = 0$	
$\lambda_2(\theta) = \dfrac{\cos\theta}{2\cos\dfrac{\alpha}{2}} - \dfrac{\sin\theta}{2\sin\dfrac{\alpha}{2}}$	$\theta = \dfrac{\alpha}{2} \rightarrow \lambda_2 = 0$ $\theta = -\dfrac{\alpha}{2} \rightarrow \lambda_2 = 1$	
$\varphi_1(\theta) = \dfrac{1}{2} + \dfrac{\sin\theta - \theta\cos\dfrac{\alpha}{2}}{2(\sin\dfrac{\alpha}{2} - \dfrac{\alpha}{2}\cos\dfrac{\alpha}{2})}$	$\theta = \dfrac{\alpha}{2} \rightarrow \varphi_1 = 1; \dfrac{\partial\varphi_1}{\partial\theta} = 0$ $\theta = -\dfrac{\alpha}{2} \rightarrow \varphi_1 = 0; \dfrac{\partial\varphi_1}{\partial\theta} = 0$	
$\varphi_2(\theta) = \dfrac{1}{2} - \dfrac{\sin\theta - \theta\cos\dfrac{\alpha}{2}}{2(\sin\dfrac{\alpha}{2} - \dfrac{\alpha}{2}\cos\dfrac{\alpha}{2})}$	$\theta = \dfrac{\alpha}{2} \rightarrow \varphi_2 = 0; \dfrac{\partial\varphi_2}{\partial\theta} = 0$ $\theta = -\dfrac{\alpha}{2} \rightarrow \varphi_2 = 1; \dfrac{\partial\varphi_2}{\partial\theta} = 0$	
$\psi_1(\theta) = \dfrac{\theta\sin\dfrac{\alpha}{2} - \dfrac{\alpha}{2}\sin\theta}{2(\sin\dfrac{\alpha}{2} - \dfrac{\alpha}{2}\cos\dfrac{\alpha}{2})}$ $+ \dfrac{\cos\dfrac{\alpha}{2} - \cos\theta}{2\sin\dfrac{\alpha}{2}}$	$\theta = \dfrac{\alpha}{2} \rightarrow \psi_1 = 0; \dfrac{\partial\psi_1}{\partial\theta} = 1$ $\theta = -\dfrac{\alpha}{2} \rightarrow \psi_1 = 0; \dfrac{\partial\psi_1}{\partial\theta} = 0$	

Table 1 Continued

$$\psi_2(\theta) = \frac{\theta \sin\frac{\alpha}{2} - \frac{\alpha}{2}\sin\theta}{2(\sin\frac{\alpha}{2} - \frac{\alpha}{2}\cos\frac{\alpha}{2})}$$

$$\theta = \frac{\alpha}{2} \rightarrow \psi_2 = 0; \frac{\partial\psi_2}{\partial\theta} = 0$$

$$-\frac{\cos\frac{\alpha}{2} - \cos\theta}{2\sin\frac{\alpha}{2}}$$

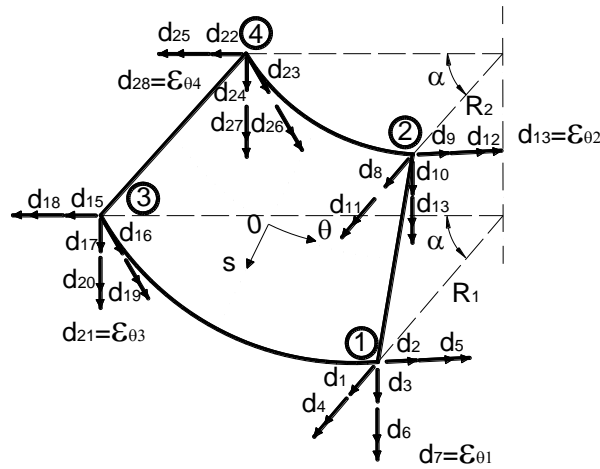$$\theta = -\frac{\alpha}{2} \rightarrow \psi_2 = 0; \frac{\partial\psi_2}{\partial\theta} = 1$$

Fig. 3 28 DOF curved shell finite element

The relation between the displacement parameters of any node of the element and the displacement and rotation components at curvilinear coordinates of that node is

$$\begin{bmatrix} u \\ v \\ w \\ \beta_\theta \\ \beta_s \\ \beta_n = \dfrac{\partial u}{r\partial\theta} \\ \varepsilon_\theta \end{bmatrix}_i = \begin{bmatrix} \cos\phi & 0 & \sin\phi & 0 & 0 & 0 & 0 \\ 0 & 1 & 0 & 0 & 0 & 0 & 0 \\ -\sin\phi & 0 & \cos\phi & 0 & 0 & 0 & 0 \\ 0 & 0 & 0 & \cos\phi & 0 & \sin\phi & 0 \\ 0 & 0 & 0 & 0 & 1 & 0 & 0 \\ 0 & 0 & 0 & -\sin\phi & 0 & \cos\phi & 0 \\ 0 & 0 & 0 & 0 & 0 & 0 & 1 \end{bmatrix} \begin{bmatrix} d_1 \\ d_2 \\ d_3 \\ d_4 \\ d_5 \\ d_6 \\ d_7 \end{bmatrix}_i \tag{3}$$

The expression which relates the distribution of the displacement components to the element freedoms is

$$[v]_e = \begin{bmatrix} u \\ v \\ w \end{bmatrix} = [A_d][d] \tag{4}$$

$[A_d]^T$ matrix is given below as

$$[A_d]^T = \begin{bmatrix}
l_1(s)\varphi_1(\theta)\cos\phi & -l_1(s)\psi_1(\theta) & -f_1(s)\varphi_1(\theta)\sin\phi \\
l_1(s)\psi_1(\theta)\cos\phi & l_1(s)\varphi_1(\theta) & -f_1(s)\psi_1(\theta)\sin\phi \\
l_1(s)\varphi_1(\theta)\sin\phi & 0 & f_1(s)\varphi_1(\theta)\cos\phi \\
-l_1(s)\psi_1(\theta)r\sin\phi & 0 & -[rf_1(s)-\cos\phi g_1(s)]\psi_1(\theta)\cos\phi \\
0 & 0 & g_1(s)\lambda_1(\theta) \\
l_1(s)\psi_1(\theta)r\cos\phi & 0 & -[rf_1(s)-\cos\phi g_1(s)]\psi_1(\theta)\sin\phi \\
0 & l_1(s)r\psi_1(\theta) & 0 \\
l_2(s)\varphi_1(\theta)\cos\phi & -l_2(s)\psi_1(\theta) & -f_2(s)\varphi_1(\theta)\sin\phi \\
l_2(s)\psi_1(\theta)\cos\phi & l_2(s)\varphi_1(\theta) & -f_2(s)\psi_1(\theta)\sin\phi \\
l_2(s)\varphi_1(\theta)\sin\phi & 0 & f_2(s)\varphi_1(\theta)\cos\phi \\
-l_2(s)\psi_1(\theta)r\sin\phi & 0 & -[rf_2(s)-\cos\phi g_2(s)]\psi_1(\theta)\cos\phi \\
0 & 0 & g_2(s)\lambda_1(\theta) \\
l_2(s)\psi_1(\theta)r\cos\phi & 0 & -[rf_2(s)-\cos\phi g_2(s)]\psi_1(\theta)\sin\phi \\
0 & l_2(s)r\psi_1(\theta) & 0 \\
l_1(s)\varphi_2(\theta)\cos\phi & -l_1(s)\psi_2(\theta) & -f_1(s)\varphi_2(\theta)\sin\phi \\
l_1(s)\psi_2(\theta)\cos\phi & l_1(s)\varphi_2(\theta) & -f_1(s)\psi_2(\theta)\sin\phi \\
l_1(s)\varphi_2(\theta)\sin\phi & 0 & f_1(s)\varphi_2(\theta)\cos\phi \\
-l_1(s)\psi_2(\theta)r\sin\phi & 0 & -[rf_1(s)-\cos\phi g_1(s)]\psi_2(\theta)\cos\phi \\
0 & 0 & g_1(s)\lambda_2(\theta) \\
l_1(s)\psi_2(\theta)r\cos\phi & 0 & -[rf_1(s)-\cos\phi g_1(s)]\psi_2(\theta)\sin\phi \\
0 & l_1(s)r\psi_2(\theta) & 0 \\
l_2(s)\varphi_2(\theta)\cos\phi & -l_2(s)\psi_2(\theta) & -f_2(s)\varphi_2(\theta)\sin\phi \\
l_2(s)\psi_2(\theta)\cos\phi & l_2(s)\varphi_2(\theta) & -f_2(s)\psi_2(\theta)\sin\phi \\
l_2(s)\varphi_2(\theta)\sin\phi & 0 & f_2(s)\varphi_2(\theta)\cos\phi \\
-l_2(s)\psi_2(\theta)r\sin\phi & 0 & -[rf_2(s)-\cos\phi g_2(s)]\psi_2(\theta)\cos\phi \\
0 & 0 & g_2(s)\lambda_2(\theta) \\
l_2(s)\psi_2(\theta)r\cos\phi & 0 & -[rf_2(s)-\cos\phi g_2(s)]\psi_2(\theta)\sin\phi \\
0 & l_2(s)r\psi_2(\theta) & 0
\end{bmatrix} \quad (5)$$

Element displacement functions entirely satisfy the rigid displacement criterion for all 6 rigid movement components. In order to check this, nodal displacement functions are expressed in terms of these components as

$$[d]_i = \begin{bmatrix} 0 & \sin\theta_i & -\cos\theta_i & 0 & -r_i\cos\theta_i\tan\phi & -r_i\sin\theta_i\tan\phi \\ 0 & \cos\theta_i & \sin\theta_i & -r_i & r_i\sin\theta_i\tan\phi & -r_i\cos\theta_i\tan\phi \\ 1 & 0 & 0 & 0 & r_i\cos\theta_i & r_i\sin\theta_i \\ 0 & 0 & 0 & 0 & \sin\theta_i & -\cos\theta_i \\ 0 & 0 & 0 & 0 & \cos\theta_i & \sin\theta_i \\ 0 & 0 & 0 & 1 & 0 & 0 \\ 0 & 0 & 0 & 0 & 0 & 0 \end{bmatrix} \cdot \begin{bmatrix} \delta_x \\ \delta_y \\ \delta_z \\ \theta_x \\ \theta_y \\ \theta_z \end{bmatrix}_i \tag{6}$$

Here, the nodal values of θ_i and r_i should be taken at every node and Eq. (2) is obtained by multiplying these values by $[A_d]$ matrix.

2.2 Internal force-displacement relations

Bending moments M_θ and torsional moments $M_{s\theta}$ are negligible for curved box girder bridges in longitudinal direction. Therefore, the curvatures corresponding to these effects are not taken into account.

The continuum strain-displacement relations in matrix form are

$$[\varepsilon] = \begin{bmatrix} \varepsilon_s \\ \varepsilon_\theta \\ \gamma_s \\ \chi_s \end{bmatrix} = \begin{bmatrix} \dfrac{\partial}{\partial s} & 0 & 0 \\ \dfrac{\cos\phi}{r} & \dfrac{\partial}{r\partial\theta} & -\dfrac{\sin\phi}{r} \\ \dfrac{\partial}{r\partial\theta} & \dfrac{\partial}{\partial s} - \dfrac{\cos\phi}{r} & 0 \\ 0 & 0 & -\dfrac{\partial^2}{\partial s^2} \end{bmatrix} \cdot \begin{bmatrix} u \\ v \\ w \end{bmatrix} \tag{7}$$

The relation between the strains and the nodal DOF is given by

$$[\varepsilon] = [B][d] \tag{8}$$

where

$$[B] = [\partial][A_d] \tag{9}$$

and

$$[\partial] = \begin{bmatrix} \dfrac{\partial}{\partial s} & 0 & 0 \\ \dfrac{\cos\phi}{r} & \dfrac{\partial}{r\partial\theta} & -\dfrac{\sin\phi}{r} \\ \dfrac{\partial}{r\partial\theta} & \dfrac{\partial}{\partial s} - \dfrac{\cos\phi}{r} & 0 \\ 0 & 0 & -\dfrac{\partial^2}{\partial s^2} \end{bmatrix} \tag{10}$$

Element internal forces can be collected in vector form as

$$[N] = \begin{bmatrix} N_s \\ N_\theta \\ N_{s\theta} \\ M_s \end{bmatrix} \tag{11}$$

so that the internal force-strain relation can be written as

$$[N] = [D][\varepsilon] \tag{12}$$

with the assumption of linear elastic material.

2.3 Stiffness matrix of shell finite element

The terms of the element stiffness matrix $[k_e]$ for the elements with constant section can be obtained by using the virtual work theorem as

$$k_{eij} = \iint \frac{Eh}{(1-v^2)} \left\{ \begin{array}{l} \dfrac{\partial u_i}{\partial s}\dfrac{\partial u_j}{\partial s} + (\dfrac{u_i}{r}\cos\phi - \dfrac{w_i}{r}\sin\phi + \dfrac{\partial v_i}{r\partial\theta})(\dfrac{u_j}{r}\cos\phi - \dfrac{w_j}{r}\sin\phi + \dfrac{\partial v_j}{r\partial\theta}) \\[2mm] + v[\dfrac{\partial u_i}{\partial s}(\dfrac{u_j}{r}\cos\phi - \dfrac{w_j}{r}\sin\phi + \dfrac{\partial v_j}{r\partial\theta}) + \dfrac{\partial u_j}{\partial s}(\dfrac{u_i}{r}\cos\phi - \dfrac{w_i}{r}\sin\phi + \dfrac{\partial v_i}{r\partial\theta})] \\[2mm] + (\dfrac{1-v}{2})(\dfrac{\partial u_i}{r\partial\theta} + \dfrac{\partial v_i}{\partial s} - \dfrac{v_i}{r}\cos\phi)(\dfrac{\partial u_j}{r\partial\theta} + \dfrac{\partial v_j}{\partial s} - \dfrac{v_j}{r}\cos\phi) + \dfrac{h^2}{12}\dfrac{\partial^2 w_i}{\partial s^2}\dfrac{\partial^2 w_j}{\partial s^2} \end{array} \right\} rdsd\theta \tag{13}$$

However, due to the complicated and long terms, Gauss integration is used to obtain the stiffness matrices of the elements with constant and variable sections.

Thus, the numerical evaluation of the stiffness matrix terms is written as

$$k_{eij} = \sum_{f=1}^{F}\sum_{g=1}^{G} H_f H_g \frac{a\alpha r}{4}\frac{Eh}{(1-v^2)} \left\{ \begin{array}{l} \dfrac{\partial u_i}{\partial s}\dfrac{\partial u_j}{\partial s} + (\dfrac{u_i}{r}cos\phi - \dfrac{w_i}{r}sin\phi + \dfrac{\partial v_i}{r\partial\theta}) \\[2mm] (\dfrac{u_j}{r}cos\phi - \dfrac{w_j}{r}sin\phi + \dfrac{\partial v_j}{r\partial\theta}) \\[2mm] + v[\dfrac{\partial u_i}{\partial s}(\dfrac{u_j}{r}cos\phi - \dfrac{w_j}{r}sin\phi + \dfrac{\partial v_j}{r\partial\theta}) \\[2mm] + \dfrac{\partial u_j}{\partial s}(\dfrac{u_i}{r}cos\phi - \dfrac{w_i}{r}sin\phi + \dfrac{\partial v_i}{r\partial\theta})] \\[2mm] + (\dfrac{1-v}{2})(\dfrac{\partial u_i}{r\partial\theta} + \dfrac{\partial v_i}{\partial s} - \dfrac{v_i}{r}cos\phi)(\dfrac{\partial u_j}{r\partial\theta} + \dfrac{\partial v_j}{\partial s} - \dfrac{v_j}{r}cos\phi) \\[2mm] + \dfrac{h^2}{12}\dfrac{\partial^2 w_i}{\partial s^2}\dfrac{\partial^2 w_j}{\partial s^2} \end{array} \right\}_{\substack{s=f \\ \theta=g}} \tag{14}$$

Here, F and G are the number of integration points used in s and θ directions, respectively, and

H_f and H_g are the weight coefficients corresponding to these points.

2.4 Second order stiffness matrix

The stiffness matrix terms of the second order effects can be expressed as

$$k_{ij}^{II} = \iint \left\{ \begin{array}{l} N_s(\dfrac{\partial v_i}{\partial s}\dfrac{\partial v_j}{\partial s} + \dfrac{\partial w_i}{\partial s}\dfrac{\partial w_j}{\partial s}) + N_\theta(\dfrac{\partial u_i}{r\partial\theta} - \dfrac{v_i}{r}\cos\phi)(\dfrac{\partial u_j}{r\partial\theta} - \dfrac{v_j}{r}\cos\phi) \\ + N_\theta(\dfrac{\partial w_i}{r\partial\theta} + \dfrac{v_i}{r}\sin\phi)(\dfrac{\partial w_j}{r\partial\theta} + \dfrac{v_j}{r}\sin\phi) \end{array} \right\} r\,ds\,d\theta \qquad (15)$$

using virtual work theorem. Here, N_s and N_θ are the membrane internal force components in s and θ directions, respectively.

Using again Gauss integration, this formulation turns to

$$k_{ij}^{II} = \sum_{f=1}^{F}\sum_{g=1}^{G} H_f H_g \frac{a\alpha\, r}{4}\left\{ \begin{array}{l} N_s(\dfrac{\partial v_i}{\partial s}\dfrac{\partial v_j}{\partial s} + \dfrac{\partial w_i}{\partial s}\dfrac{\partial w_j}{\partial s}) + N_\theta(\dfrac{\partial u_i}{r\partial\theta} - \dfrac{v_i}{r}\cos\phi)(\dfrac{\partial u_j}{r\partial\theta} - \dfrac{v_j}{r}\cos\phi) \\ + N_\theta(\dfrac{\partial w_i}{r\partial\theta} + \dfrac{v_i}{r}\sin\phi)(\dfrac{\partial w_j}{r\partial\theta} + \dfrac{v_j}{r}\sin\phi) \end{array} \right\}_{\substack{s=f \\ \theta=g}} \qquad (16)$$

The element stiffness matrix including the second order effects is obtained by taking the sum of the first order terms and the additional second order terms as

$$\left[K_e^{II}\right] = [K_e] + \left[K^{II}\right] \qquad (17)$$

3. Numerical tests

3.1 Box-girder beam with curved axis

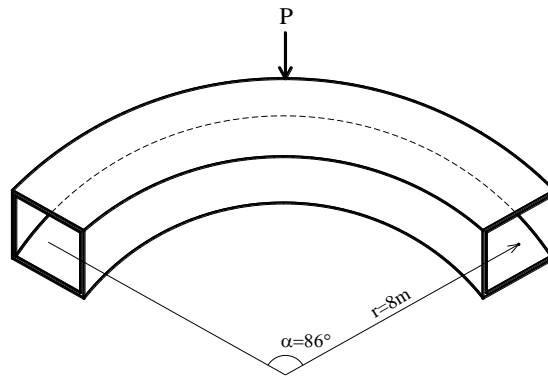A simply supported steel box-girder beam with curved axis is studied. The geometry and
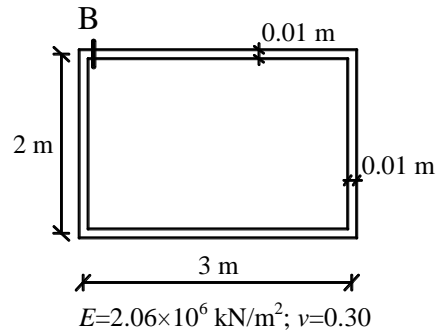

Fig. 4 Curved box-girder beam

$E=2.06\times10^6$ kN/m^2; v=0.30

Fig. 5 Curved box-girder beam cross-section

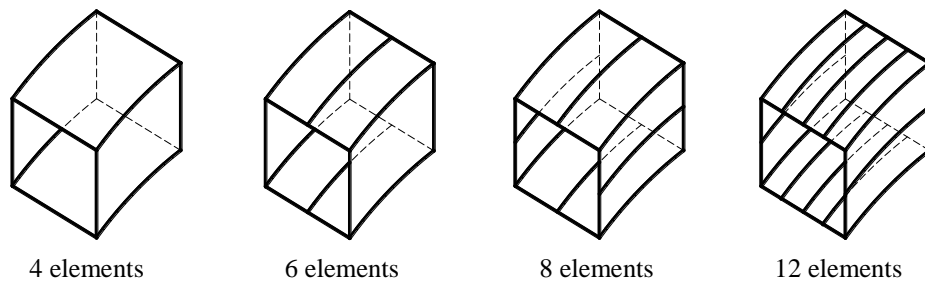4 elements   6 elements   8 elements   12 elements
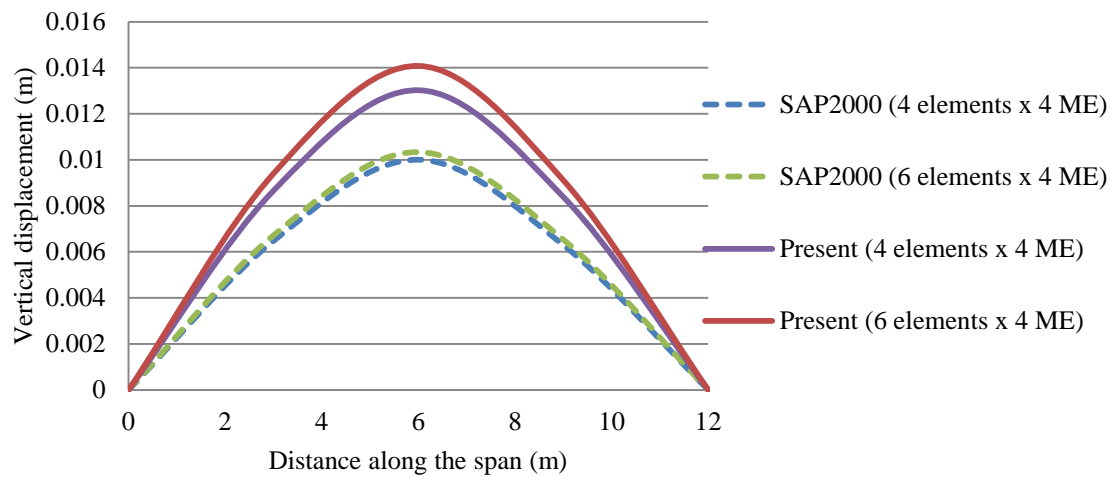
Fig. 6 Macro-element models

Fig. 7 Vertical displacements along the beam using 4 ME

material properties of the system are given in Figs. 4-5. The beam which is subjected to an eccentric vertical point load of P=1000 kN at the midspan is modelled by the proposed shell finite element and SAP2000 using various number and 4 different types of macro-elements as shown in Fig. 6.

First, the beam is modelled using 4 ME with 4 and 6 elements at each ME. The obtained vertical displacements of the top left corner along the beam are comparatively plotted in Fig. 7. Displacements increase as the number of elements increase from 4 to 6 and it is obvious that there is a relatively significant difference between the results of the present study and those of SAP2000.

The same system is then modelled using 10 ME by SAP2000 and the results are compared to the results of the present study with 4 ME as given in Fig. 8. The displacements of SAP2000 are closer but still not satisfactory.

Finally, the system is analysed by SAP2000 refining the meshes from 4 to 30 ME having different number of elements at each ME. It is seen from Fig. 9 that the most convergent results upon mesh refinement are obtained by using the proposed shell finite element only with 4 ME having 6 elements at each ME. Close results by SAP2000 are obtained when 30 ME with 12 elements at each are used.
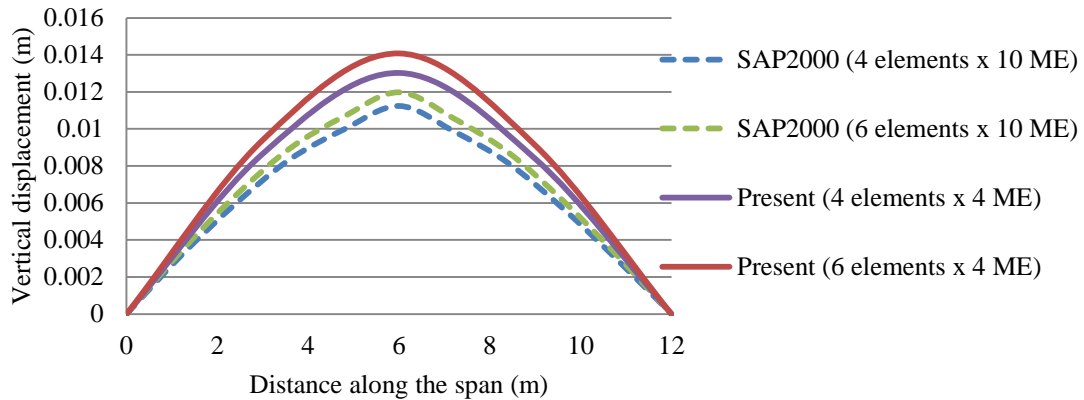

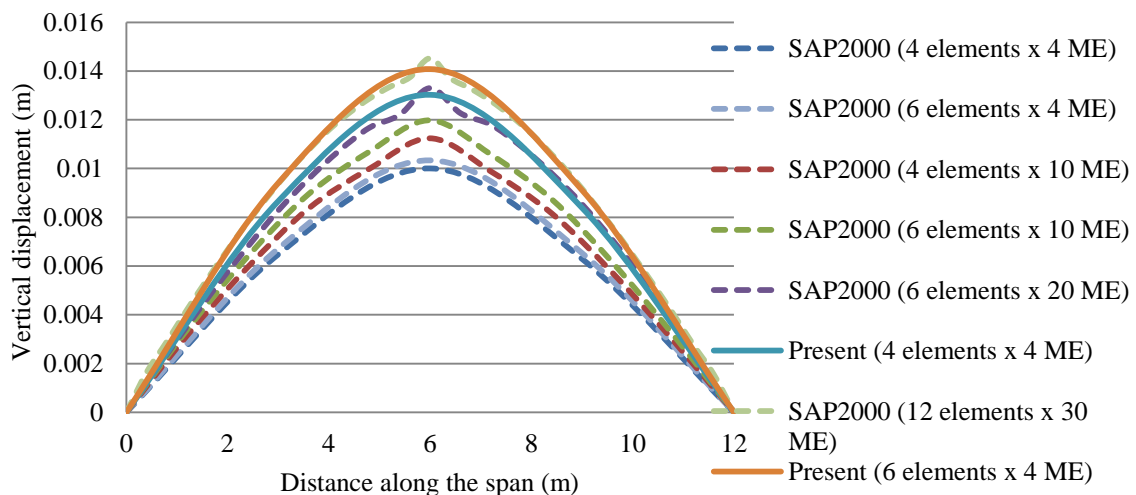Fig. 8 Vertical displacements along the beam using 4 and 10 ME

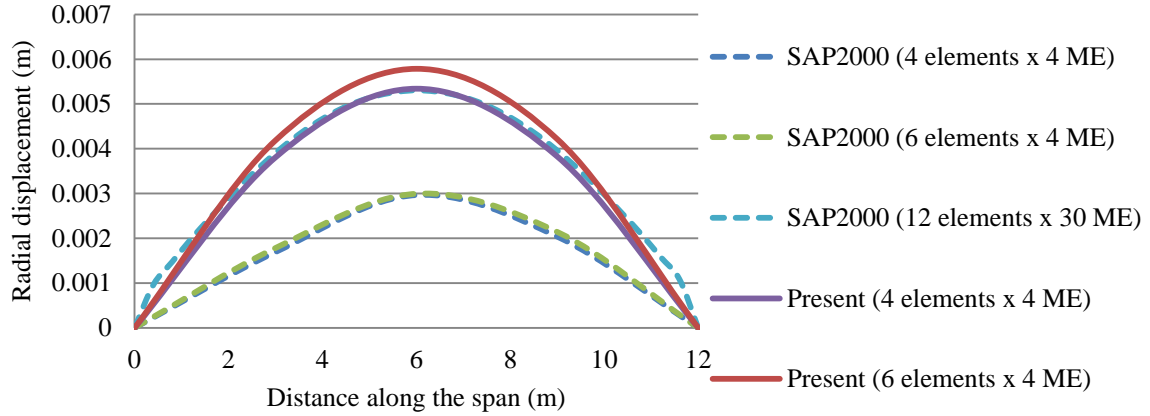Fig. 9 Vertical displacements along the beam using various number of ME
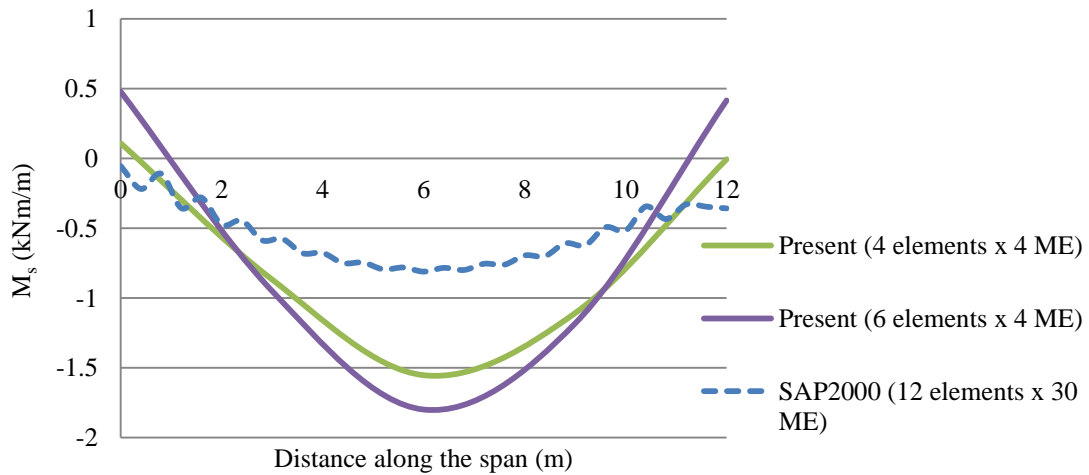
Fig. 10 Radial displacements along the beam

Fig. 11 Bending moments in the radial direction

Radial displacements of the curved box-girder beam are also examined. It is observed from Fig. 10 that the results of the present study using a very coarse mesh (4 elements × 4 ME) and SAP2000 using a fine mesh (12 elements × 30 ME) show good agreement. Coarse mesh results of SAP2000 are very far from the others and the displacement curve obtained by using the present shell element modelled with 6 elements x 4 ME is the most satisfactory of all.

In addition to the displacements, internal forces of the curved beam are examined. Bending moment values of section B in radial direction obtained using the proposed shell element and SAP2000 are comparatively given in Fig. 11 and it is seen that the moment values of the present study decrease as the number of elements per ME increase and satisfactory results cannot be achieved even by the usage of a fine mesh in SAP2000.

Normal forces at section B in the radial direction which are expected to be zero along the beam can be achieved using 8 elements × 10 ME of the present shell element while 12 elements × 30
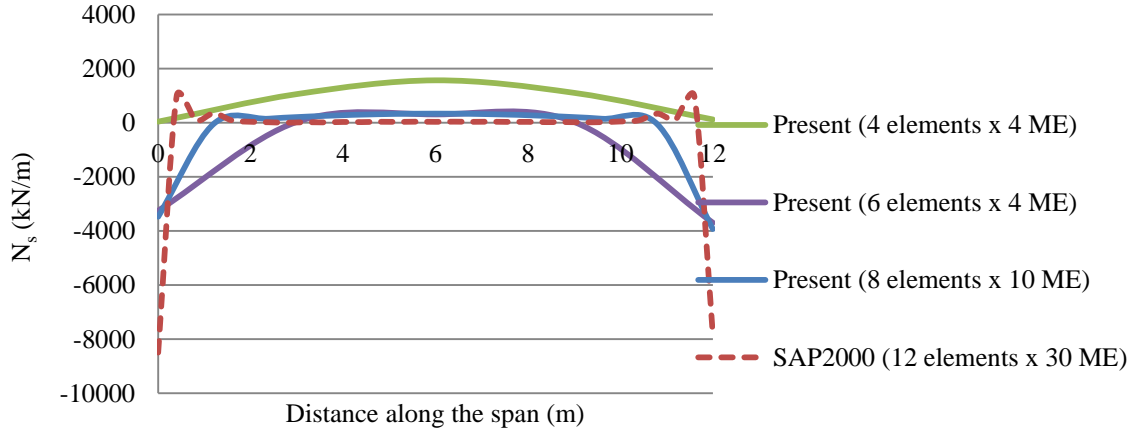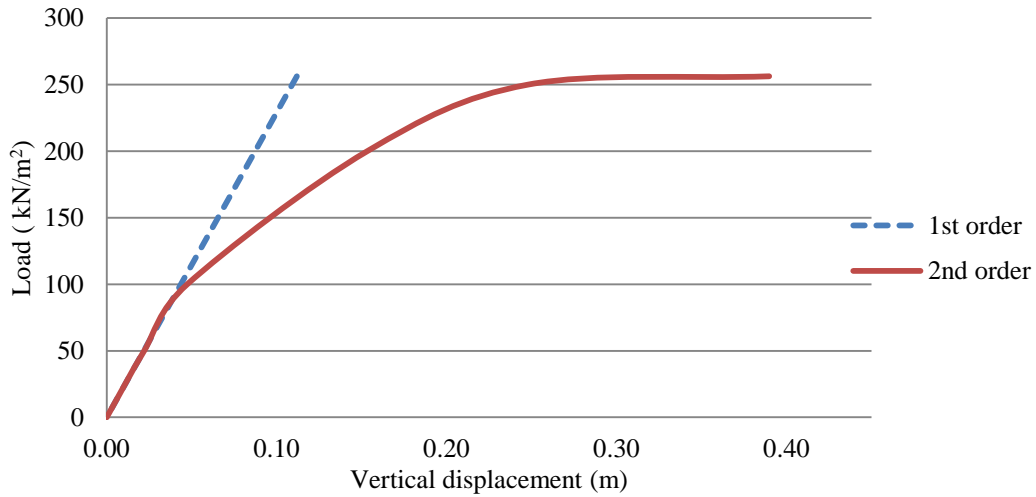
Fig. 12 Normal forces in the radial direction

Fig. 13 Vertical displacements at the midspan obtained in the first and the second order theories

ME are used in SAP2000 analysis in order to obtain zero values. 6 elements × 4 ME results using the proposed shell element are also satisfactory, Fig. 12.

The curved box-girder beam is then subjected to increasing uniformly distributed loads in vertical direction and linear and geometrically non-linear analyses are carried out. 10 ME and 8 elements per ME are used in the analyses. A straight line is obtained via the first order solutions as expected and it is seen that the rate of vertical displacements increase with the load increment when nonlinearities are taken into account. The vertical displacements at the midspan increase by 3.5 times with the maximum applied load of 256.25 kN/m^2, cf. Fig. 13.
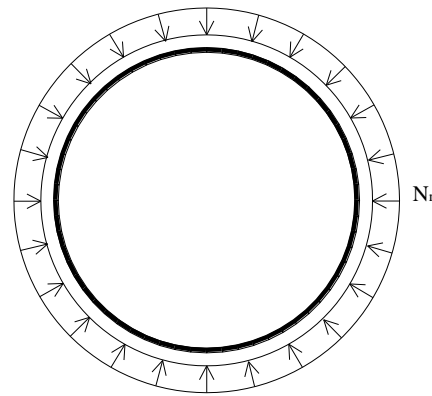
3.2 Circular plate

Secondly, a circular plate example subjected to a uniform radial compression is studied. The

geometry and material properties of the system are given in Fig. 14 where h is the thickness and a is the radius. The system is analysed for two different support conditions which are simple and clamped supports. In modelling, a ring sector finite element is used which is obtained by setting the slope angle of the curved shell finite element to 0°, and a very small hole is assumed to be at the centre of the plate in order to avoid singularities. The in-plane pressure is idealized with equivalent P_1 and P_2 point forces acting on the boundary nodes of different meshes as shown in Fig. 15. Buckling loads are obtained for all mesh refinements and also analytically as given in Timoshenko and Gere (1961), and all results are given comparatively in Table 2 and Fig. 16.

The critical pressure of the clamped circular plate can be obtained analytically as in Timoshenko and Gere (1961) using

$$N_{cr} = 14.68 \frac{Eh^3}{12(1-v^2)a^2} = 1004 \text{ kN/m} \tag{18}$$

$E = 21 \times 10^7$ kN/m^2; $v = 0.30$

$h = 0.02$ m; $a = 1.50$ m

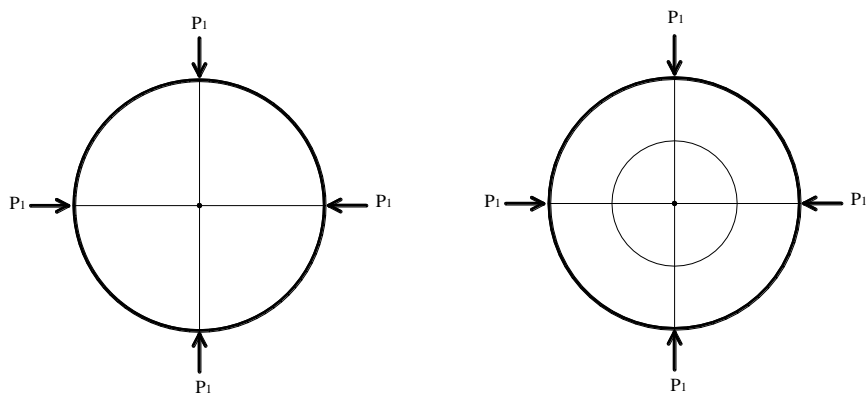Fig. 14 Circular plate under uniform in-plane pressure

Fig. 15 Circular plates with various meshes

Fig. 15 Continued
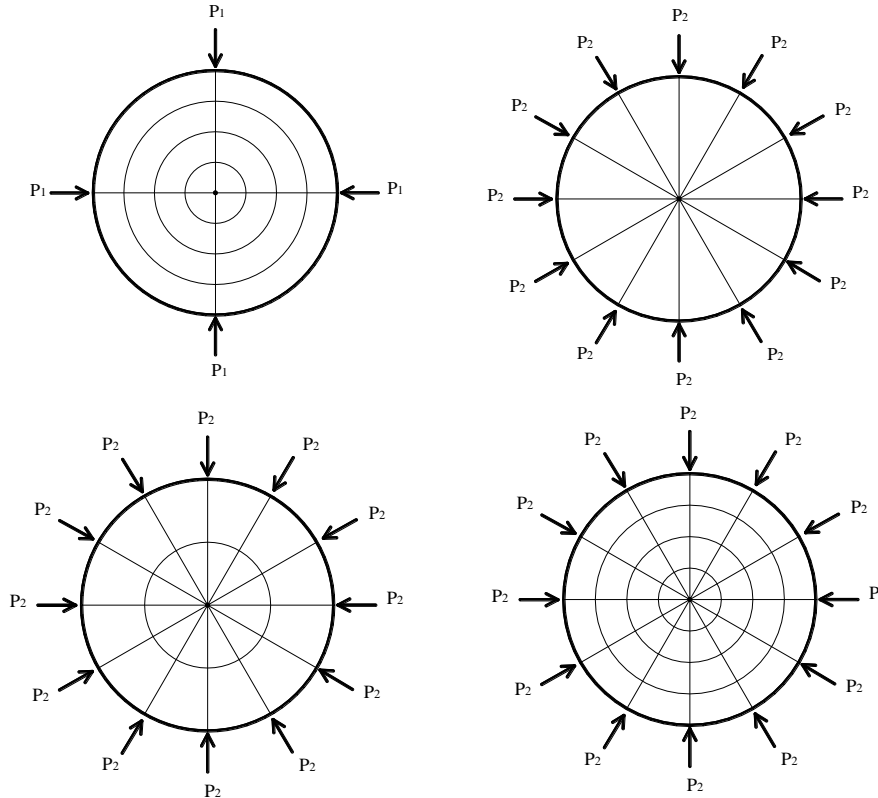
Table 2 Comparison of buckling loads of circular plate

	Buckling load (kN/m)				
	4 elements	8 elements	16 elements	32 elements	Analytical
Simply supported	404	336	304	298	287
Clamped	1022	1172	1069	1031	1004

The critical pressure of the simply supported circular plate is obtained analytically as in Timoshenko and Gere (1961) via

$$N_{cr} = 0.425\pi^2 \frac{Eh^3}{12(1-v^2)a^2} = 287\,\text{kN/m} \tag{19}$$

As seen from the results, the buckling loads of the circular plate rapidly converge to the analytical solution upon mesh refinement. Satisfactory results are obtained for the simply supported circular plate even by using a very coarse mesh (4 elements). However, the usage of 4 elements for the plate with clamped support does not give satisfactory results due to the buckling mode of the plate. It is seen that the buckling load of a clamped circular plate increases about 3.5 times compared to the simply supported circular plate. It is also observed that refining the meshes in angular direction causes only a minor change in the results.
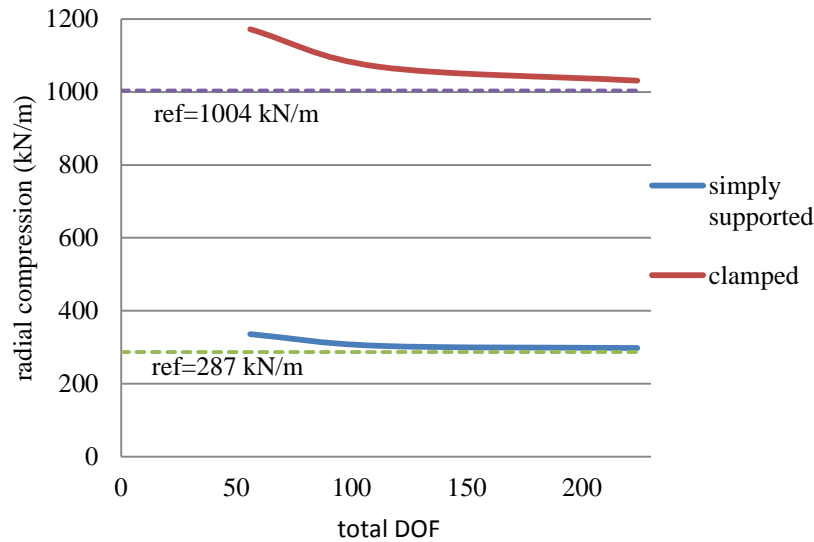
Fig. 16 Comparison of buckling loads of a circular plate

4. Conclusions

In this paper, a four-noded curved shell finite element with second order effects is introduced. It is demonstrated that curved box-girder beams can be realistically modelled and satisfactory results can be obtained even by using coarse meshes of the proposed shell finite element.

Firstly, a steel curved box-girder beam example is analysed. The vertical and radial displacements and the internal forces of the system due to an eccentric load of 1000 kN are obtained both by SAP2000 and by using the proposed shell element. It is observed from the results that satisfactory results can be obtained even by using very coarse meshes of the present shell element while fine meshes need to be used by SAP2000 for that purpose.

Geometrically non-linear analyses of the beams with curved shape can also be made by the inclusion of the second order effects to the curved shell finite element formulation. The curved beam is then analysed under increasing distributed loads both according to the first and second order theories. It is observed that the effects of the geometrical nonlinearities gain importance with the load increment, e.g., the vertical displacements at the midspan increase by 3.5 times with the maximum applied load of 256.25 kN/m^2.

Finally, a circular plate example subjected to a uniform radial pressure is studied. The buckling loads of the circular plate converge to the analytical solutions even by using very coarse meshes. The buckling load increases about 3.5 times by changing the support conditions from clamped to simple and it can be said that refining the meshes in angular direction does not change the results.

References

Erkmen, R.E. and Bradford, M.A. (2009), "Nonlinear elastic analysis of composite beams curved in plan", *Eng. Struct.*, **31**, 1613-1624.

Fam, A.R.M. and Turkstra, C.J. (1975), "A finite element scheme for box girder analysis", *Comput. Struct.*, **5**, 179-186.

Hall, H.D. (1996), "Curved girders are special", *Eng. Struct.*, **18**(10), 769-777.

Hiroshi, N. and Chai, H. (1988), *Analysis and Design of Curved Steel Bridges*, McHill Book Company, New York, NY.

Hsu, Y.T., Fu, C.C. and Schelling, D.R. (1990), "An improved horizontally curved beam element", *Comput. Struct.*, **34**(2), 313-318.

Meyer, C. and Scordelis, A.C. (1971), "Analysis of curved folded plate structures", *J. Struct. Div.*, ASCE, **97**(10), 2459-2480.

Moffat, K.R. and Lim, P.T.K. (1977), "Some finite elements having particular application to box girder bridges", *IABSE Proceedings*.

Park, N.H., Choi, S. and Kang, Y.J. (2005), "Exact distortional behaviour and practical distortional analysis of multicell box girders using an expanded method", *Comput. Struct.*, **83**, 1607-1626.

Razaqpur, A.G. and Li, H. (1991), "Thin-walled multicell box-girder finite element", *J. Struct. Eng.*, **117**, 2953-2971.

Razaqpur, A.G. and Li, H.G. (1994), "Refined analysis of curved thin-walled multicell box girders", *Comput. Struct.*, **53**, 131-142.

Razaqpur, A.G. and Li, H.G. (1997), "Analysis of curved multicell box girder assemblages", *Struct. Eng. Mech.*, **5**(1), 33-49.

Shanmugam, N.E., Thevendran, V., Liew, J.Y.R. and Tan, L.O. (1995), "Experimental study on steel beams curved in plan", *J. Struct. Eng.*, ASCE, **121**(2), 249-259.

Timoshenko, S.P. and Gere, J.M. (1961), *Theory of Elastic Stability*, McGraw-Hill.

Vo, T.P. and Lee, J. (2009), "Geometrically nonlinear analysis of thin-walled composite box beams", *Comput. Struct.*, **87**, 236-245.

Vo, T.P. and Lee, J. (2010), "Geometrically nonlinear analysis of thin-walled open-section composite beams", *Comput. Struct.*, **88**, 347-356.

Wang, R.H., Li, Q.S., Wu, J.R. and Tang, J. (2005), "A spatial elastic displacement model for curved box girders with corner stiffeners", *Comput. Struct.*, **83**, 1021-1029.

Wang, X. and Yang, Q. (2009), "Geometrically nonlinear finite element model of spatial thin-walled beams with general open cross section", *Acta Mechanica Solida Sinica*, **22**(1), 64-72.

Zhang, S.H. and Lyons, L.P.R. (1984), "A thin-walled box beam finite element for curved bridge analysis", *Comput. Struct.*, **18**(6), 1035-1046.

Zureick, A., Linzell, D., Leon, R.T. and Burrell, J. (2000), "Curved steel I-girder bridges: experimental and analytical studies", *Eng. Struct.*, **22**, 180-190.